Alignment of energy levels at the $Alq_3/La_{0.7}Sr_{0.3}MnO_3$ interface for organic spintronic devices

Y. Q. Zhan,* I. Bergenti, L. E. Hueso, and V. Dediu
Istituto per lo Studio di Materiali Nanostrutturati, Consiglio Nazionale delle Ricerche (ISMN-CNR), via Gobetti 101, 40129 Bologna, Italy

M. P. de Jong
Department of Physics, IFM, Linköping University, S-581 83 Linköping, Sweden

Z. S. Li
Institute for Storage Ring Facilities, University of Aarhus, Ny Munkegade, Building 1520, DK 8000 Aarhus C, Denmark
(Received 8 March 2007; published 11 July 2007)

The electronic structure of the interface between tris(8-hydroxyquinolino)-aluminum (Alq_3) and $La_{0.7}Sr_{0.3}MnO_3$ (LSMO) manganite was investigated by means of photoelectron spectroscopy. As demonstrated recently, this interface is characterized by efficient spin injection in organic spintronic devices. We detected a strong interface dipole of about 0.9 eV that shifts down the whole energy diagram of the Alq_3 with respect to the vacuum level. This modifies the height of the barrier for the injection into highest occupied molecular orbital level to 1.7 eV, indicating more difficult hole injection at this interface than expected for the undistorted energy level diagram. We believe that the interface dipole is due to the intrinsic dipole moment of the Alq_3 layer. The presented data lead to significant progress in understanding the electronic structure of LSMO/Alq_3 interface and represent a step toward the description of spin transport in organic spin valves.

DOI: 10.1103/PhysRevB.76.045406 PACS number(s): 73.21.−b, 72.25.Mk, 72.80.Le

In the past few decades, the field of organic electronics has progressed enormously, stimulated by the availability of a virtually infinite number of organic molecules, each with a unique electronic and optical property. While the efforts have been mainly concentrated on the control of charges in various devices, the interest toward spin manipulation in such materials has considerably grown recently. Due to the weak spin-orbit and hyperfine interactions in organic π-conjugated semiconductors, the spin coherence in most organic semiconductors (OS) is expected to be robust and propagate to longer distances than in conventional metals and semiconductors. The first Communication on spin injection in OS reported room temperature magnetoresistance in sexithiophene (T6) connected to two manganite [$La_{0.7}Sr_{0.3}MnO_3$ (LSMO)] electrodes[1] and real spin-valve effects were reported in tris(8-hydroxyquinolino)-aluminum (Alq_3) confined in a vertical geometry between manganite (bottom) and Co (top) electrodes.[2] Recently spin-valve effects have been confirmed for various vertical manganite-Alq_3 based devices.[3,4] A spin tunneling across thin Alq_3 layer was recently demonstrated to persist up to room temperature.[5] Most of the successful organic devices for spintronic applications were so far based on a combination of Alq_3 as OS and manganite thin films as spin polarized injectors. While the bulk and even surface properties of these materials are well understood, the information of their interface, the key region for both charge and spin injections, is completely lacking. A few publications related to interfaces interesting for spintronic applications have dealt with totally different cases such as Alq_3/Co,[6] C60/Co,[7] and pentacene/Co.[8,9]

In this paper, we investigate the Alq_3/LSMO interface by photoelectron spectroscopy (PES). The samples consist of Alq_3 thin films of various thicknesses deposited *in situ* on LSMO bottom layer. The valence band spectra and secondary electron cutoffs of the Alq_3/LSMO interface, as well as the core level spectra of both LSMO and Alq_3, have been studied in order to obtain the detailed energetics of this interface.

Experiments were carried out using the SX700 beamline at the ASTRID synchrotron source (ISA, Denmark) with photon energies in the 60–600 eV range at room temperature. Electrons were analyzed using a VG CLAM II (30 eV pass energy). Spectra were obtained at normal emission with respect to sample surfaces, and the angle between incident photon beam and direction of the analyzer detection was 45°. The overall resolution was about 0.1 eV. Each spectrum was normalized by the primary photon flux obtained by recording continuously the primary beam intensity on a gold grid. Both valence band spectra and secondary electron cutoffs of Alq_3 on LSMO were obtained with a photon energy of 60 eV. The photon energies of 600 and 145 eV were used to investigate the N 1*s* and Al 1*p* levels of Alq_3. Also, a bias voltage of V_b=−9.4 V was applied to the sample during the secondary binding energy cutoff measurements in order to distinguish between analyzer and sample cutoffs. An evaporation chamber was connected to the analysis chamber, in which the predeposited LSMO films were covered *in situ* by a thin Alq_3 film. Both analysis and evaporation chambers were baked before the experiments; after baking, the background pressures were 8×10^{-10} and 8×10^{-8} mbar, respectively.

A series of 20 nm thick LSMO films was deposited on matching $NdGaO_3$ substrates by using the pulsed electron deposition (in the pulsed plasma deposition configuration).[10] During the deposition, the substrates were heated to 800–850 °C, while the oxygen pressure was kept at 10^{-2} mbar. This procedure ensures high quality epitaxial LSMO films with high Curie temperature ($T_C\sim320$–340 K, depending on film thicknesses) and a resistivity lower than 10 mΩ cm at 300 K. The surface electronic and magnetic

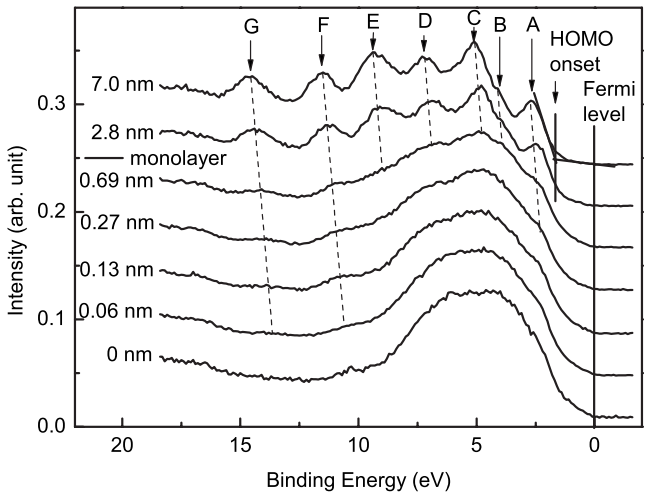

FIG. 1. Valence band photoelectron spectra at the Alq_3/LSMO interface.

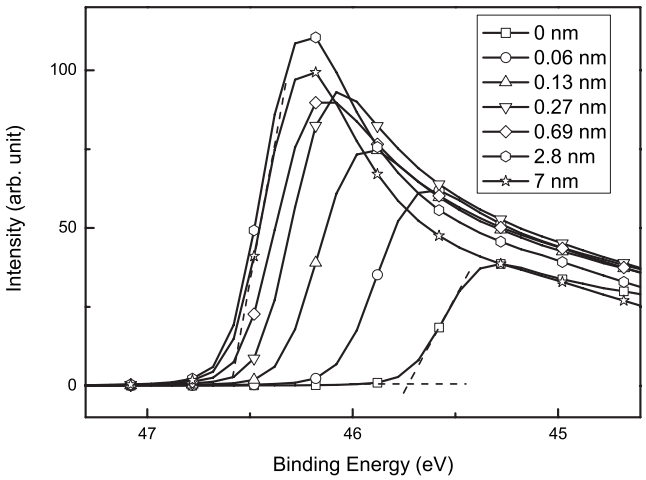

FIG. 2. Secondary electron cutoffs of Alq_3 on LSMO.

properties of our films were characterized in detail by various techniques.[11–13]

The LSMO substrates (5×10 mm^2) were introduced in the evaporation chamber after a rinse with ethanol in an ultrasonic bath. The samples were annealed in UHV and subsequently in a 2×10^{-5} mbar oxygen atmosphere for 30 min at 500 °C. These procedures were found to remove the surface carbon contamination and to restore the surface oxygen stoichiometry without impacting the overall bulk properties of the films.[14] Such oxygen annealing (450–500 °C) is well known and does not change the low-energy electron diffraction patterns and the x-ray photoemission spectroscopy (XPS) spectra of the manganite film surfaces.[15]

The Alq_3 films were grown following a step by step sublimation of the organic material from a Knudsen cell at 235 °C. At few chosen thicknesses, the deposition was interrupted and the sample was transferred to the PES chamber. Subsequently, after PES characterization, the sample is transferred back to the deposition place. The thicknesses were calibrated by deposition time and confirmed later by *ex situ* atomic force microscopy measurements.

In Fig. 1, the valence band spectra of Alq_3 on LSMO are shown as a function of its thickness from 0 to 7 nm, where 0 nm of Alq_3 corresponds to the investigation of the bare LSMO substrate. Reproducible results were obtained on all three investigated samples.

The photoemission spectrum of LSMO (0 nm) presents distinct metallic behavior with a broad peak in the 2–8 eV region related to O $2p$ and Mn $3d$ photoelectron emission near the Fermi level.[11] Since LSMO does not have a very sharp Fermi edge, the Fermi edge of cobalt was used as reference to calibrate the energy scale.

As the Alq_3 thickness increases, the emission from the LSMO substrate becomes suppressed and the spectrum continuously changes toward that of Alq_3. The 7 nm Alq_3 film represents already the typical bulk Alq_3 spectrum: seven distinct Alq_3 molecular features, in agreement with published reports,[16,17] occur at binding energies of 2.6 (A), 4.0 (B), 5.0 (C), 7.2 (D), 9.3 (E), 11.4 (F), and 14.5 (G) eV. Structures A and B have been assigned to electron emission from the $2p$ σ and π orbitals of the 8-quinolinol ligands of Alq_3. The nature of other peaks is still debated.[16]

The Alq_3 highest occupied molecular orbital (HOMO) peak corresponds to feature A which is the nearest peak to the Fermi level. The HOMO energy onset was defined by the intersection of the tangent line of the HOMO peak with the base line of the Alq_3 spectrum. In the 7 nm thick film, the HOMO onset of Alq_3 is located at $E_{\mathrm{HOMO}}=1.7$ eV below Fermi level; the relative position of the HOMO energy onset from the LSMO Fermi level is thus defined by the comparison of spectra corresponding to 0 and 7 nm.

The evolution of the interface is described by the valence band variations at different Alq_3 coverages. The spectrum corresponding to 0.06 nm Alq_3 is similar to that of the pure LSMO, indicating the major contribution of the substrate except a tiny shoulder raised at the position of 2.4 eV. By increasing the thickness to 0.13 nm, the features of Alq_3's valence band become evident, especially for the peaks F and G which are not overlapped by the large and broad valence band peak of LSMO. Features A–E also become evident by further increasing the Alq_3 thickness; the whole Alq_3 valence band is clearly seen in the spectrum corresponding to an Alq_3 thickness of 2.8 nm, which is about two monolayers.[18,19]

By comparing the peak position of each feature, a significant shift toward lower binding energy with increasing the thickness of Alq_3 can be observed. The dashed lines, which connect the peaks of the same feature, are parallel, indicating a synchronous shift. By measuring intersections between the dashed line of feature G for 0.06 and 7 nm Alq_3 spectra, an energy shift of about 0.9 eV is found. Since all the peaks in Alq_3 valence band are referenced to the Fermi energy of LSMO, the $\Delta=0.9$ eV shift should be related to a modification of the LSMO work function while depositing Alq_3.

The ultrathin nature of the analyzed Alq_3 films ensures that the sample charging is negligible, making the determination of the work function from the secondary electron cutoff energy reliable (Fig. 2). Alternatively, upon growing the full thickness of the organic films, measurements as Kelvin probe may represent a complementary technique for the surface analysis. Let us first analyze the 0 nm curve in Fig. 2, corresponding to bare LSMO surface. The work func-

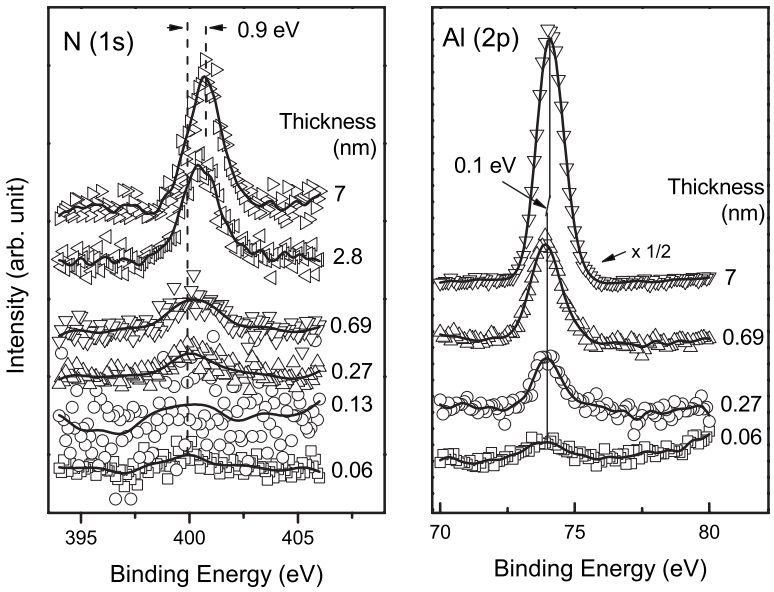

FIG. 3. Photoelectron spectra of N 1 *s* and Al 2*p* levels at the Alq_3/LSMO interface.

tion of the LSMO substrate is calculated as $\phi_{LSMO}=4.9$ eV in agreement with our previous data.[13] The Alq_3 deposition leads to a strong decrease of the work function, and, finally for the thick Alq_3 film corresponding to 7 nm thickness, the cutoff is shifted to higher energy by $\Delta_\phi=-0.9$ eV. This value corresponds exactly to the shift found for the valence band features and unambiguously indicates the presence of a strong interfacial dipole. The origin of such a dipole layer can be attributed to several factors: charge transfer across the interface,[20] Pauli repulsion,[21,22] strong chemical interaction,[23] and oriented permanent molecular dipoles.[24] Considering that depositing Alq_3 lowers the work function, the corresponding interfacial dipole has its positive pole pointing out of the surface. This allows us to exclude a charge transfer mechanism from Alq_3 to LSMO because the high ionization potential of Alq_3 (5.7 eV) prevents any electron transfer from Alq_3 to LSMO. Pauli repulsion can be large for high work function metals featuring a large surface dipole contribution to the work function, but it is expected to be rather small for LSMO. This is because in LSMO, the 3*d* electron density is low compared to that of the 3*d* transition metals, leading to a correspondingly low electron density leaking out into the vacuum.[25,26]

By far, the most likely explanation of the observed dipole is that it stems mainly from the permanent dipole of Alq_3, which is rather large: 4 D for the meridional isomer and 7 D for the facial isomer.[27] Such a scenario requires a preferred adsorption geometry at the first layer, induced by the LSMO-Alq_3 interaction, which should align the individual dipoles of the adsorbates in a way similar to the one observed for Alq_3 on Al.[28,29] The effects of additional layers on top of the first adsorbate, either crystalline or amorphous, are indeed minor, as follows from the saturation of the work function above a certain films thickness.

A simple estimation of the work function modification $\Delta\phi$ (in eV) upon adsorbing an areal density n of molecules (m^{-2}), each carrying a dipole moment μ (in C m), can be obtained from the Helmholtz equation $\Delta\phi=\mu n/(\varepsilon_0\varepsilon)$. Here, ε is the dielectric constant at the interface, determined by the polarizabilities of both Alq_3 and LSMO. For a complete densely packed monolayer, we can estimate the areal density as 2.5×10^{18} m^{-2} based on an average lattice constant of Alq_3 crystals of about 1 nm (x-ray diffraction data[18]). Assuming a dielectric constant of about 4,[30] an average dipole of 4 D per molecule (the value for the most common meridional isomer) would give approximately a 1 eV shift, which fits our experimental results very well. Alternatively, depolarization effects might play a role at high coverages. Such effects have been observed in many adsorbate systems and are traditionally interpreted in the framework of the Topping model.[31]

It is worth pointing out that a strong decrease of the work function upon deposition of Alq_3 molecules is generally observed, independently of the substrate and its initial work function. Examples that can be found in the literature include Cu and Au,[32] Au,[33] Al, and LiF/Al.[24,34] The insensitivity to the specific substrate indicates that indeed the main contribution to the interfacial dipole must stem from the intrinsic dipole of Alq_3. Since the Alq_3 molecules are most likely to interact with any substrate through two of its ligands instead of only one, partial ordering of the molecular dipoles might be expected, although this has not been demonstrated so far.

In order to explore the possible interaction at the interface of Alq_3/LSMO, a set of XPS measurements for core levels was performed. Figure 3 shows the evolutions of the N (1*s*) and Al (2*p*) core levels upon deposition of Alq_3 on LSMO. Following the initial Alq_3 deposition, the N (1*s*) component develops at 399.8 eV. Upon increasing the thickness of Alq_3, the N (1*s*) peak is more and more clear and a shift of 0.9 eV to the lower energy is evidenced, in analogy with the shifts observed in the valence band spectra. Since the peak of the very thin Alq_3 can be considered as coming from interface while the thick one represents the bulk, this shift is in line with the previously discussed interfacial dipole, shifting the N (1*s*) to higher binding energy by about 0.9 eV. It is very important to note that the core level spectra of all LSMO elements indicated no observable modification upon varying the Alq_3 film thickness.

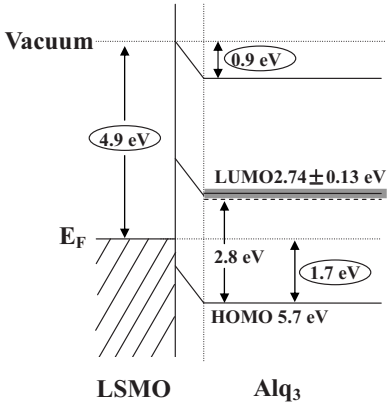

FIG. 4. Schematic energy band diagram of the Alq_3/LSMO interface. The values directly measured in our experiments are evidenced by circles; the optical gap (2.8 eV) between the dashed line and the HOMO is taken from Ref. 30 and the LUMO level (2.74±0.13 eV) is calculated from STS data (Refs. 33 and 34).

In Al (2*p*) spectra, on the other hand, a much smaller shift can be evidenced. The Al (2*p*) component remains at 74 eV until the thickness of Alq_3 increases to 0.69 nm. Between 0.69 and 7 nm, a 0.1 eV shift is visible.

From Figs. 1 and 2, we can obtain the electronic structure of the interface between Alq_3 and LSMO (Fig. 4). Based on Fig. 2, the vacuum level of Alq_3 is 0.9 eV lower than the vacuum level of bare LSMO, which is placed at 4.9 eV above the Fermi level. The HOMO level of Alq_3 is 1.7 eV lower than the LSMO Fermi level. Thus, the ionization potential of Alq_3 is 4.9−0.9+1.7=5.7 eV, which is similar to the reported literature data.[35]

The energy of the lowest unoccupied molecular orbital (LUMO) edge of the Alq_3 layer can be deduced from the energy of the HOMO edge and the HOMO-LUMO splitting. We are interested in a diagram able to describe the charge (spin) injection at this interface. It is quite common to use the optical gap of 2.8 eV (Ref. 35) for the calculation of the LUMO energy.[33,35,36] Nevertheless, such a definition does not take into account the excitonic binding energy that should somehow increase the real energy of the LUMO level as far as the carrier injection is concerned.

The methods which allow us to measure or estimate the single particle band gap are the inversed photoemission spectroscopy (IPES), scanning tunneling spectroscopy (STS), and transport measurements (*IV* curves), although the latter requires the exact knowledge of the transport mechanism. The IPES techniques give quite high values for the single particle gap—up to 4.6–5.2 eV.[37] Such a high value is in strong contradiction with most transport characterizations of the Alq_3 based organic light-emitting diodes[38] and could be caused by the sample modification under the strong flux of electrons. The STS measurements of the empty states provide, on the other hand, a completely nonperturbative method, as it operates at vanishingly low currents (10^{-12} A). A direct STS measured HOMO-LUMO splitting (2.96±0.13 eV) has been reported by Alvarado *et al.*[39,40] This value was confirmed to describe well the charge injection barrier in light-emitting diodes.[38] The absolute value of the LUMO level in our diagram can thus be calculated as 2.74±0.13 eV. It provides the 1.26±0.13 eV barrier height for the electron injection (from the Fermi level to LUMO level of Alq_3), in good agreement with literature data[38] and with our own calculations (1 eV).[4]

According to this diagram, the hole injection barrier is much larger than it would have been expected considering the vacuum level alignment.[2,3] On the other hand, electron injection barrier is smaller. The possibility of electron injection should certainly be considered in the devices involving the LSMO/Alq_3 interface. This statement is of great importance for understanding the spin-valve behavior and could be the key issue for the high spin injection efficiency observed at this interface.

In conclusion, the electronic structure of the Alq_3/LSMO interface was investigated by means of photoelectron spectroscopy. We detected a strong interface dipole of about 0.9 eV that shifts down the whole energy diagram of the Alq_3 with respect to the vacuum level. This modifies the height of the barriers for the holes and electrons injection to 1.7 and 1.26±0.13 eV, respectively. The intrinsic dipole moment characteristic for Alq_3 molecules seems to be the most probable origin of the observed interface dipole, in line with previously reported Alq_3/metal interfaces. We believe these results are of greatest importance for the quantitative description of LSMO/Alq_3 based organic spintronic devices.

ACKNOWLEDGMENT

The authors acknowledge financial support from EU OFSPIN project.

*yq.zhan@bo.ismn.cnr.it

[1] V. Dediu, M. Murgia, F. C. Matacotta, C. Taliani, and S. Barbanera, Solid State Commun. **122**, 181 (2002).
[2] Z. H. Xiong, D. Wu, Z. V. Vardeny, and J. Shi, Nature (London) **427**, 821 (2004).
[3] S. Majumdar, H. S. Majumdar, R. Laiho, and R. Osterbacka, J. Alloys Compd. **423**, 169 (2006).
[4] A. Riminucci, I. Bergenti, L. E. Hueso, M. Murgia, C. Taliani, Y. Zhan, F. Casoli, M. P. de Jong, and V. Dediu, arXiv:cond-mat/0701603.
[5] T. S. Santos, J. S. Lee, P. Migdal, I. C. Lekshmi, B. Satpati, and J. S. Moodera, Phys. Rev. Lett. **98**, 016601 (2007).
[6] A. N. Caruso, D. L. Schulz, and P. A. Dowben, Chem. Phys. Lett. **413**, 321 (2005).
[7] J. H. Seo, S. J. Kang, C. Y. Kim, K. H. Yoo, and C. N. Whang, J. Phys.: Condens. Matter **18**, S2055 (2006).
[8] M. V. Tiba, W. J. M. de Jonge, B. Koopmans, and H. T. Jonkman, J. Appl. Phys. **100**, 093707 (2006).
[9] M. Popinciuc, H. T. Jonkman, and B. J. van Wees, J. Appl. Phys. **100**, 093714 (2006).

[10] V. A. Dediu, J. Lopez, F. C. Matacotta, P. Nozar, G. Ruani, R. Zamboni, and C. Taliani, Phys. Status Solidi B **215**, 625 (1999).
[11] M. P. de Jong, I. Bergenti, W. Osikowicz, R. Friedlein, V. A. Dediu, C. Taliani, and W. R. Salaneck, Phys. Rev. B **73**, 052403 (2006).
[12] M. P. de Jong, I. Bergenti, V. A. Dediu, M. Fahlman, M. Marsi, and C. Taliani, Phys. Rev. B **71**, 014434 (2005).
[13] M. P. de Jong, V. A. Dediu, C. Taliani, and W. R. Salaneck, J. Appl. Phys. **94**, 7292 (2003).
[14] K. Horiba, A. Chikamatsu, H. Kumigashira, M. Oshima, N. Nakagawa, M. Lippmaa, K. Ono, M. Kawasaki, and H. Koinuma, Phys. Rev. B **71**, 155420 (2005).
[15] J. W. Choi, J. D. Zhang, S. H. Liou, P. A. Dowben, and E. W. Plummer, Phys. Rev. B **59**, 13453 (1999).
[16] K. Sugiyama, D. Yoshimura, T. Miyamae, T. Miyazaki, H. Ishii, Y. Ouchi, and K. Seki, J. Appl. Phys. **83**, 4928 (1998).
[17] T. W. Pi, T. C. Yu, C. P. Ouyang, J. F. Wen, and H. L. Hsu, Phys. Rev. B **71**, 205310 (2005).
[18] J. F. Moulin, M. Brinkmann, A. Thierry, and J. C. Wittmann, Adv. Mater. (Weinheim, Ger.) **14**, 436 (2002).
[19] X. M. Ding, L. M. Hung, C. S. Lee, and S. T. Lee, Phys. Rev. B **60**, 13291 (1999).
[20] I. G. Hill, A. Rajagopal, A. Kahn, and Y. Hu, Appl. Phys. Lett. **73**, 662 (1998).
[21] J. L. F. Da Silva, C. Stampfl, and M. Scheffler, Phys. Rev. Lett. **90**, 066104 (2003).
[22] V. De Renzi, R. Rousseau, D. Marchetto, R. Biagi, S. Scandolo, and U. del Pennino, Phys. Rev. Lett. **95**, 046804 (2005).
[23] G. Heimel, L. Romaner, J. L. Bredas, and E. Zojer, Phys. Rev. Lett. **96**, 196806 (2006).
[24] H. Ishii, K. Sugiyama, E. Ito, and K. Seki, Adv. Mater. (Weinheim, Ger.) **11**, 605 (1999).
[25] R. M. Nieminen and C. H. Hodges, J. Phys. F: Met. Phys. **6**, 573 (1976).
[26] H. L. Skriver and N. M. Rosengaard, Phys. Rev. B **46**, 7157 (1992).
[27] A. Curioni, M. Boero, and W. Andreoni, Chem. Phys. Lett. **294**, 263 (1998).
[28] D. Ino, K. Watanabe, N. Takagi, and Y. Matsumoto, Phys. Rev. B **71**, 115427 (2005).
[29] S. Yanagisawa and Y. Morikawa, Jpn. J. Appl. Phys., Part 1 **45**, 413 (2006).
[30] S. Berleb and W. Brütting, Phys. Rev. Lett. **89**, 286601 (2002).
[31] J. Topping, Proc. R. Soc. London, Ser. A **114**, 67 (1927).
[32] D. Ino, K. Watanabe, N. Takagi, and Y. Matsumoto, Phys. Rev. B **71**, 115427 (2005).
[33] I. G. Hill, A. J. Makinen, and Z. H. Kafafi, Appl. Phys. Lett. **77**, 1825 (2000).
[34] S. K. M. Jonsson, W. R. Salaneck, and M. Fahlman, J. Appl. Phys. **98**, 014901 (2005).
[35] S. T. Lee, X. Y. Hou, M. G. Mason, and C. W. Tang, Appl. Phys. Lett. **72**, 1593 (1998).
[36] T. Mori, H. Fujikawa, S. Tokito, and Y. Taga, Appl. Phys. Lett. **73**, 2763 (1998).
[37] I. G. Hill, A. Kahn, Z. G. Soos, and R. A. Pascal, Chem. Phys. Lett. **327**, 181 (2000).
[38] U. Wolf, S. Barth, and H. Bassler, Appl. Phys. Lett. **75**, 2035 (1999).
[39] S. F. Alvarado, L. Rossi, P. Muller, P. F. Seidler, and W. Riess, IBM J. Res. Dev. **45**, 89 (2001).
[40] S. F. Alvarado, L. Libioulle, and P. F. Seidler, Synth. Met. **91**, 69 (1997).